Volume 1 | Number 1 | Jan 2013 | Pages 1–100

PCCP

Physical Chemistry Chemical Physics
www.rsc.org/pccp

ROYAL SOCIETY OF CHEMISTRY

ROYAL SOCIETY OF CHEMISTRY

www.rsc.org/pccp

Journal Name

Physical Chemistry Chemical Physics

ARTICLE TYPE

Correlation between thermodynamic properties, thermal expansion and electrical resistivity of Ag – 28 % Cu nanopowders processed by mechanical alloying route

Speranta Tanasescu,*[a] Alexandru Milea,[a] Oana Gingu,[b] Florentina Maxim[a], Cristian Hornoiu[a], Silviu Preda[a], and Gabriela Sima[b]

Thermodynamic properties, thermal expansion and electrical resistivity of the Ag – 28 % Cu nanopowders processed by mechanical alloying route have been investigated in the temperature range from ambient to 1048 K. The thermodynamic properties represented by the relative enthalpy, the specific heat capacity, relative entropy and Gibbs energy function obtained from drop calorimetric measurements have been used to reveal the occurrence of the micro-relaxation process, as well as of the correlative effects of decomposition and growth processes. On the basis of the results, the parameters that favor stable nanostructured systems in Ag – 28 % Cu powders synthesized by mechanical alloying route have been identified. The correlation of the energetic parameters with thermal expansion and electrical resistivity in mechanical alloyed nanocrystalline powders with the eutectic composition is discussed.

1. Introduction

Much attention has been generated by nanoalloys obtained through nonequilibrium processing routes like rapid quenching from liquid state,[1] vapor deposition,[2] ion beam mixing,[3,4] DC sputtering,[5,6] plasma processing[7] or ball milling of elemental powders[8,9]. The novel properties and applications of these materials compared to their equilibrium counterparts provide new opportunities for technological applications ranging from electronic to catalytic, magnetic and optic applications.[10-15]

At the same time, the possibility to obtain metastable nanoscale alloys present challenges as concern the understanding of the phase formation and stability. By the combined use of molecular dynamics (MD) simulations and experimental characterizations employing local-environment probes, it was shown that alloy phase transformation can proceed under different constraints and via different mechanisms being strongly correlated with the processing parameters, the composition, the homogeneity and local structural features in the alloy.[5,16]

Ag-Cu is one of the nanoalloy systems which have received considerable attention for both applicative and fundamental reasons.[10] It is well known that Ag and Cu are mutually immiscible in the solid state under equilibrium conditions, and exhibit positive heat of mixing.[17] Even though these alloys did not easily synthesized by conventional casting, however they can now be produced through far from equilibrium processing techniques, such as vapor deposition and mechanical alloying.[18-21] Previous studies on metastable Ag-Cu alloys report that solid solutions, amorphous or nanocrystalline phases can be produced depending on the processing conditions.

Even though has been emphasized that the phase formation would be strongly correlated with the structure and energetics of the competing phases, the thermodynamics and mechanisms underlying the phase transformations induced by the nonequilibrium processing methods are still not well understood.

The calculations of the thermodynamic functions for metastable phases in Ag-Cu system by using models and methods like CALPHAD approach, Miedema model, free energy minimization and embedded atom methods (FEMM/EAM) remain difficult and sometimes unreliable if the input data are limited to the equilibrium conditions.

To experimentally investigate the thermal behavior of the Ag-Cu nanoalloys produced by mechanical alloying, differential scanning calorimetry has been generally used. Excepting our recent work,[22] the previous publications on thermal behavior cover only restricted temperature ranges, generally until approximately 673-773 K.[14,16,20,23] By combining modeling approach with differential scanning calorimetry, some information has been obtained regarding the enthalpy-composition curves for metastable phases over limited composition domain.[5,16,24,25] Despite the amount of research being conducted on this area, the experimental information on the relevant functions suitable for thermodynamic evaluations of chemical processes of phase formation associated with a specific processing technique it is still scarce and need to be investigated.

It has been a goal of our recent work[22] to identify the characteristic system parameters that favour stable nanostructured systems in Ag - 28% Cu powders synthesized by mechanical alloying route. By a critical comparison of the isothermal enthalpy (obtained by drop calorimetric measurements) with dynamic DSC results and in situ controlled annealing XRD

experiments, a key output of our prior work[22] was a preliminary understanding of the thermodynamic stability correlation with the effect of the milling time and particle size in a large temperature range from room temperature to 1073 K.

Continuing this study, the goal of the present paper is to provide new experimental thermodynamic, thermal expansion and electrical data aiming to identify the parameters that favour stable nanostructured systems in Ag - 28% Cu powders synthesized by mechanical alloying route. Of particular interest for us is to evidence the role of the thermodynamic properties in controlling grain size stability of nanocrystalline material with eutectic composition. New features related to the correlation of the energetic parameters with thermal expansion and electrical properties in nanocrystalline Ag - 28% Cu powders obtained by mechanical alloying are discussed.

2. Experimental

2.1. Materials and sample preparation

The eutectic composition mixture Ag+28% wt. Cu has been processed by mechanical alloying (MA) route, starting from powders of Ag (Sigma Aldrich ≥ 99,9%) and Cu (Sigma Aldrich 99%). The powders were mixed in appropriate amounts in a planetary ball mill Pulverisette 6 (Fritsch, Germany) under protective argon atmosphere. The used milling vial and balls are from agate in order to avoid the powder contamination during the MA processing. The detailed technological parameters (rotation speed balls milling dimensions, balls/powder ratio) are described elsewhere.[26]

2.2 Sample characterization

The structure of the sample after milling, as well as with subsequent controlled annealing, was studied by powder X-ray diffraction (PXRD) using a Rigaku Ultima IV diffractometer. The procedure was described in detail in our previous paper.[22] *In-situ* XRD measurements were performed using the same equipment and parameters, in continuous mode, from 323 to 973 K, in open air atmosphere. The crystallite size was estimated by Scherrer equation from broadening of (111) diffraction line of Ag–Cu$_{ss}$, using the formula[27]:

$$\frac{1}{d^2} = \frac{h^2 + k^2 + l^2}{a^2} \qquad (1)$$

where D is the mean size of the ordered crystalline domains, which may be smaller or equal to the grain size; K = 0.94 is a dimensionless shape factor or Scherrer constant; λ is the X-ray wavelength; β is the line broadening at half the maximum intensity (FWHM), in radians and θ is the Bragg angle.

The particles morphology, primary size and the elemental analysis were analyzed by scanning electron microscopy (SEM) with a FEI Quanta 3D FEG microscope equipped with energy-dispersive X-ray detector (EDX).

The enthalpy increments H_T-H_{298} of the sample in isothermal regime were investigated by drop calorimetry using a multi-detector high temperature calorimeter (MHTC-96) of SETARAM working in the drop mode. Ag-Cu powder was pressed into small pellets weighing about 60–100 mg and was dried up to 393 K in vacuum in order to remove any water adsorbed on the surface of nanosized powders. The experiments consist in dropping a sample kept at room temperature into a pure α - alumina bed maintained at a desired temperature ($T \pm 0.1$ K). Isothermal measurements were performed in argon atmosphere by alternate dropping of the reference material (small pieces of synthetic sapphire, NIST Standard Reference Material no. 720) and the sample pellets. For the stabilization of temperature and heat flux, between the drops a time interval of about 30 min is provided. In a typical experiment, three samples of α-alumina reference material and three samples of Ag-Cu have been dropped. Enthalpy increments were calculated using the following expression:

$$(H_T - H_{298})_s = \frac{\int Q_s dT}{Q_R dT} \cdot \frac{M_S}{m_s} \cdot \frac{m_R}{M_R} \cdot (H_T - H_{298})_R \qquad (2)$$

where Q_R and Q_S stand for the drop calorimetry signal obtained at a fixed temperature T with either reference (R) or sample (S) under identical experimental conditions. M_R and m_R are the molar mass and mass of the α-alumina reference material and M_S and m_S are the molar mass and mass of the sample.

Thermal expansion of the samples associated with the structural changes was investigated by using a Thermomechanical analyzer SETSYS Evolution TMA calibrated to a quartz standard. The sample powder was pressed into pellets of 3 mm diameter and 1.66 mm height. A force equivalent to a weight of 5 g was applied on the sample in order to remove vibrations that could appear during experiment. Thermal expansion measurements were performed at a heating rate of 5 K/min over the range from room temperature to 973 K and in argon with a 16 ml/min gas flux.

The electrical measurements were realized using a two-probe AC impedance spectrometer with an electrochemical interface (Solartron 1260). The AC bias applied potential difference amplitude was 500 mV AC. Electrochemical Impedance spectra (EIS) were recorded in the frequency range of 2 MHz to 100 Hz from room temperature to 973 K with a ProboStat cell (NorECs, Oslo, Norway) under air atmosphere. The electrical resistivity (ρ) was determined using geometrical factors of samples:

$\rho = R_{meas} A/l$, where R_{meas} is the measured electrical resistance, l - length of the piece of material and A - cross-sectional area. The electrical resistivity values were corrected for thermal expansion using our thermal expansion data. The corrected value ($\rho_{corrected}$), was obtained by the relation:[28]

$$\rho_{corrected}(T) = \left(1 + \frac{\Delta L(T)}{L_0}\right)\rho_{corrected}(T) \qquad (3)$$

where $\Delta L = L$-L_0, and L and L_0 are the lengths of the specimen at any temperature T and the length of the specimen at the room temperature, respectively. The thermal expansion correction amount is about 0.5 % to 7 % in the temperature domain investigated.

3. Results and discussion

The SEM micograph of the Ag-Cu alloy is presented in Fig. 1a showing an aggregate of spherical nanopowders with average
5 particle size of about 30 nm. By EDX spectroscopy (Fig. 1b) it is confirmed that the nanoparticles are comprised of both Ag and Cu in the atomic ratio corresponding to the initial mixture of the metal powders. To note here that the presence of Al in the EDX spectra is due to the SEM stub used as sample support.

10
Fig. 1 a) SEM micrograph and b) EDS analysis of the Ag-28% Cu alloy nanopowders ball milled for 80 hours

The heat effects related to the thermodynamic behaviour of the
15 nanopowders Ag – 28 % Cu were evaluated by calorimetric measurements in isothermal regime using the multi-detector calorimeter SETARAM MHTC-96 operating in drop mode. The experimentally obtained enthalpy increments (H_T-H_{298}) in the temperature range of 373-1048 K are shown in Fig. 2. Because
20 the enthalpy variation with temperature is basically nonlinear in nature, the heat contents were expressed as an explicit temperature function f (T) for every temperature interval where phase transition is not revealed and least squared fitted into polynomial equations of the form:

25
$$H_T - H_{298} = a + bT + cT^2 \qquad (4)$$

The deviations of the fit values from experimental estimates are represented by a standard deviation of 0.35%. At higher temperatures, above 900 K, the standard deviation is about 1.12.

30 Fig. 2 Temperature dependence of the experimental enthalpy increments (H_T-H_{298}) and derived heat capacity (C_p) of the Ag – 28 % Cu nanopowders processed by mechanical alloying route

The temperature-dependent estimates of the heat capacity were
35 obtained by differentiating above enthalpy increment equations with respect to temperature:

$$C_P = \frac{\partial}{\partial T}(H_T - H_{298}) \qquad (5)$$

The heat capacity values obtained in this way have been also shown in Fig. 2.
40 The larger values of the enthalpy and specific heat capacities observed at lower temperatures around 400 K (Fig. 2) are explained by the nanocrystalline structure generated by high-energy ball milling. The enhancement of the specific heats with the nanocrystallinity in metals or alloys was also noticed by other
45 authors[29,30] being correlated with the weaker interatomic coupling in nanosized materials due to the more open atomic structure of the grain boundary component.[28] Between 448 and 473 K a first inflection of the enthalpy with temperature is noted, the event being associated with the relaxation of microstresses created
50 during the ball-milling process. This effect due to the larger strain energy accumulated after longer milling times has been previously reported by Spassov[14] on the DSC curves of Cu-Ag alloys milled for 12 and 20 h and has been also observed on the DSC curves of the 20 and 80 hours milled samples which were
55 discussed in our recent paper.[22] As we were expecting, this effect is followed by a steadily decreasing of heat capacity on an

interval of about 75 K. The clear inflection observed between 548 and 573 K is followed by an interval of about 50 K in which both the enthalpy increments and the heat capacity values are almost
60 constant. After 623 K, the enthalpy exhibits a gradual increase up to about 1048 K, even though, in spite of the increasing character of enthalpy, the presence of some other features is also noticed around 848, 898 and 948 K. The heat capacity it is also increasing from 623 K, but the C_p weaker temperature dependence has to be
65 noted.
In order to obtain further clarification on the relationship between the thermodynamic parameters and the structure evolution, the crystalline behavior and phase transformations of the Ag−Cu alloy nanoparticles with heating were investigated by
70 in-situ XRD measurements. The Fig. 3 shows the XRD patterns at room temperature before and after heating (see inset A of Fig. 3), as well as at representative heating temperatures, at which the phase transformations take place. For the as milled sample, the diffraction line is broad and shifted in regard to the position of
75 pure Ag (ICDD file no. 01-087-0720) (see inset A of Fig. 3), suggesting the formation of Ag-Cu solid solution (Ag-Cu$_{ss}$). By heating up to 503 K, the main diffraction line indicative of Ag-Cu solid solution it is still registered, but the presence of metallic Cu and Cu$_2$O can be identified. In the X-ray diffractograms above
80 503 K, the positions of Ag peaks almost coincide with those of un-milled Ag powders, which mean that Cu atoms dissolved in Ag almost completely precipitated. At 582 K, the presence of CuO can be noticed, that may be due to the oxidation of metallic copper and cuprite during heating. Furthermore, at 659 K, no
85 evidence of metallic copper and only trace of cuprite can be noticed. At 734 K, the phase transformation of Cu$_2$O to CuO is already completed. No other phase transformation was detected above this temperature. In the inset B of the Fig. 3, the evolution with temperature of the main diffraction line of the Ag-Cu$_{ss}$ is
90 highlighted. According to Zhu,[31] the mechanically alloyed solid solution sample could be seen on heating as a nanophase composite with Ag and Cu regarded as matrix phase and secondary phase, respectively. The shifting to higher interplanar distances (Fig. 3, inset B) can be due to cumulative effects of the
95 thermal expansion and Cu segregation from the solid solution.[22] Also, the narrowing of the diffraction line is a measure of increasing the crystallite size with temperature, indicating an apparent grain growth in the sample.

100 Fig. 3 In situ XRD of the Ag – 28 % Cu nanopowders during heating at successively increased temperature from RT to 973 K (Inset A: XRD patterns at room temperature before and after heating; Inset B: the evolution with temperature of the main diffraction line of the Ag-Cu$_{ss}$)

105
Correlating with these results, the enthalpy evolution from about 473 K to 950 K could be assigned to the alloy decomposition associated with the grain growth process. Even though the occurrence of these processes have been also noticed
110 in some other reports on different mechanically alloyed Ag-Cu materials,[14,20,23,32] as well as on Ag-Cu alloys formed by quenching (sputter deposition) and cold-rolled samples,[5] however there are a few papers trying to discriminate between the correlative effects of these processes. To our best knowledge our

report is the first work giving such information on the Ag-Cu nanopowders with the eutectic composition.

Of special interest for us is to show how the energetic parameters may be used to understand the particularities of the nanocrystalline structures behaviour at the metastable thermodynamic equilibrium.

To further evaluate the heat content evolution in the interval 473-1048 K, the enthalpy values have been least squared fitted using the following equations:

$$H_T\text{-}H_{298} \text{ (J/g)} = -415.96 + 1.65917\ T - 0.00141\ T^2 \quad (473\text{-}548 \text{ K}) \tag{6}$$

$$H_T\text{-}H_{298} \text{ (J/g)} = -41.95 + 0.1656\ T - 9.19034 \times 10^{-5}\ T^2 \quad (573\text{-}1048 \text{ K}) \tag{7}$$

By using expression (5), the heat capacities have been obtained. For the relative entropy and the free energy functions, the following relations have been used:

$$S_T - S_{298} = \int_{298}^{T} \frac{C_P}{T} dT \tag{8}$$

$$\frac{G_T - H_{298}}{T} = \frac{H_T - H_{298}}{T} - S_T \tag{9}$$

The heat capacities and the thermodynamic functions obtained by processing these equations have been included in Table 1. The precision of the values (taken as twice the standard deviation) is 0.2 % for the heat capacity and 0.15 % for the thermodynamic functions over the low temperature range; in the high temperature range they are 0.4 and 0.2%, respectively. At higher temperature these deviations can partly originate from the nature of nucleation and growth phenomenon. On heating, different samples might have experienced slightly different extents of transformation and can be inhomogeneous.

Thermodynamic data represented by heat capacity, entropy and free energy functions for Ag - 28% Cu nanopowders obtained by mechanical alloying process have not been previously reported in the literature. In the absence of other data to compare, in order to generate thermodynamic functions for bulk Ag-Cu alloy, we used in situ synthesis by direct reaction calorimetry. According to the method previously described,[22] the powders of the same elemental starting materials as used in the milling process were mixed in the given ratio and dropped from the room temperature into the calorimeter at 973 K, so they will react inside. Then, the above obtained pellet was subsequently removed and again dropped from room temperature into calorimeter to obtain the heat content of the compound. From the relative enthalpy values, the heat capacity, the relative entropy and energy function values of the bulk sample were calculated by using the previous relationships. These values have been included for comparison in Table 1. In the same table were summarized the values of the energetic parameters obtained for a sample milled for 20 hours and having the average particle size dimension of 272 nm.[22]

Table 1 Values of thermodynamic functions for Ag - 28% Cu nanometer-sized sample processed by mechanical alloying route in comparison with the thermodynamic functions values obtained for bulk and for a micrometer-sized mechanical alloyed sample with the same composition

The larger entropies obtained in the 473 – 548 K temperature interval for the nanosized milled sample comparing with the bulk and microsized sample is characteristic for the high degree of disorder present in the boundaries. The lower values of the energy function noted for this sample at temperatures around 500 K speaks in the favor of thermodynamic nanostructure stabilization. This means that after the alloy decomposition, the free energy of the system reaches a local minimum with respect to the grain growth to some critical value D_{crit}. This result is in agreement with the concept of thermodynamic nanostructure stabilization in the metastable alloys systems which has been developed in the latest years.[33-38] These investigations show that samples with smaller grain sizes have enhanced thermal stabilities, suggesting that grain growth temperature and activation energy for growth in a nanocrystalline state are higher in comparison with that in coarse grains. According to Koch,[38] only nonequilibrium processing methods such as the severe plastic deformation of mechanical alloying can induce metastable solid solution.

Several authors pointed out that binary nanocrystalline alloys could be thermodynamic stabilized by segregation of solute at the grain boundaries, leading to an equilibrium grain size at which the system energy is minimized.[39-41] In order to verify this statement for Ag - 28% Cu mechanical alloyed nanopowders, in Fig. 4, the crystallite size calculated using the Scherrer equation for (111) diffraction line registered by in-situ XRD measurements, together the energy function (Table 1) are represented as a function of heating temperature. It can be seen that no obvious dependence of grain growth on temperature occurred for nanophase composite. A small dependence of average crystallite size on heating temperature is observed until about 500 K, suggesting that the reduction in the grain boundary energy shows weak temperature dependence. At the same time a minimum in energy (Fig. 4, Table 1) and in the specific heat capacity (Table 1) is noted around 500 K. This result is in agreement with some previous studies[31,38,39] on thermal stabilization of nanocrystalline metals and alloys. When the temperature is higher than 500 K the crystallite size increases obviously with the increase of heating temperature (Fig. 4), suggesting that the equilibrium grain size decreases with increasing solute content. However it is important to mention that beginning with 573 K both energy and heat capacity of the nanosized sample show weak temperature dependence when compared with the microsized and bulk samples (Table 1). This result it is also in agreement with some authors noting that a reduction in the grain boundary energy, which shows only weak temperature dependence, might be more effective for the stabilization of nanocrystalline grain sizes at the highest temperatures.[38,42] The experimental results obtained in the present study by correlating the crystallite size with the energy function give for the first time evidence that, the concept of thermodynamic nanostructure stabilization is a real phenomenon for the mechanically alloyed nanometer-sized Ag-Cu sample with eutectic composition. The lowering of interfacial energy with grain refinement and lattice strain in nanometer-sized crystallites

plays an important role in controlling grain size stability of nanocrystalline materials during the grain growth in nanocrystalline phases.[40,43-46] Moreover, this is an important issue of research when searching alloying strategies for minimizing grain growth to be developed.[38,33-35]

Fig. 4 Crystallite size (XRD measurements) and Gibbs energy function (drop calorimetry data) of the Ag - 28% Cu mechanical alloyed nanopowders as a function of temperature

The small inflections or plateau-like characteristics in the heat capacity and enthalpy behaviour above 573 K (Fig. 2, Table 1) are indicative for occurrence of transformations related to the grain growth process as they are also accompanied by finite changes in the enthalpy content.[16] If the transformation is a nucleation and growth phenomenon, it requires some superheating to facilitate the attainment of thermodynamic equilibrium. The possible presence of such high temperature homogenization would serve to decrease or attenuate the continuously increasing trend of enthalpy and heat capacity with temperature.

Taking into account the particular behaviour of the thermodynamic properties of the nanocrystalline Ag - 28% Cu obtained by mechanical alloying, it may be expected that this sample should have a specific variation of the thermal expansion properties, as well as of the electrical resistivity. Despite the fact that these data are important in assuring the reliability of solder joints based on Ag-Cu alloys, it is a lack of thermal expansion data for this system.

Thermal expansion upon heating in Argon atmosphere for nanocrystalline Ag - 28 % Cu composition is represented in Fig. 5 and Fig. 6 together with the crystallite size (obtained from XRD measurements) and with energy function (from drop calorimetry), respectively.

Fig. 5 Temperature dependence of the thermal expansion and crystallite size of the Ag – 28 % Cu nanopowders

Fig. 6 Thermal expansion and Gibbs energy function of the Ag – 28 % Cu nanopowders as a function of temperature

As shown, the thermal expansion curve is relative linear below 450 K. Then, until 500 K, the structure relaxation seems to show negative contribution on lattice expansion. After 500 K, which is at a crystallite size near the critical value from which it was expecting the grain boundary becomes mechanically unstable (Figs. 5 and 6), the thermal expansion begins to experience a curving range, the linear displacement becoming steeper with temperature after 673 K and until 893 K. The results presented in Fig. 5 and Fig. 6 together the previous discussion on the thermodynamic properties evolution speak in the favor of the strong correlation between the thermal expansion and the energetic parameters controlling the growth process of nanometer-sized sample. The average thermal expansion coefficient (CTE) determined from our data over the temperature range 473-548 K (which is around the temperature at which the free energy of the system reaches a local minimum with respect to the grain growth) was 44 x 10^{-6} K^{-1}. Since nanocrystalline materials contain a large amount of interfacial volume, its

coefficient of thermal expansion (CTE) is expected to be higher than in a coarse-grained material.[47] Measurements of the thermal expansion of nanocrystalline Cu, Ag, Pd yielded to CTE values of about two times higher than the value of coarse-grained materials[45,48,49]. The enhancement of the thermal expansion coefficient was also reported for Ni-P alloys in going from micrometer-sized to nanometer-sized specimens[50]. Taking into account that the common values for silver alloys in bulk are in the range of about 18–20 x 10^{-6} K^{-1}, the value of 44 x 10^{-6} K^{-1} obtained by us for nanocrystalline Ag – 28 % Cu sample would agree with previous statement about the enhancement of the thermal expansion in nanocrystalline metals and alloys. To our best knowledge there are no other studies reporting the thermal expansion coefficient in Ag – 28 % Cu nanopowders.

Because of the increased volume fraction of atoms lying at the grain boundaries, the electrical resistivity of nanocrystalline materials is affected by grain boundary scattering. In turn, the increase in the scattering of charge carriers at the interfaces is caused by a high thermal expansion coefficient of the grain boundaries[48]. Investigation of the electrical resistivity of the Ag - 28% Cu sample gives new arguments when speaking about the role of the energetic parameters in explaining the particular behaviour of Ag-Cu nanopowders with eutectic composition. In Fig. 7 the changes of the relative specific resistance ρ/ρ_0 with temperature was shown for two mechanically alloyed samples with the same composition (Ag – 28 % Cu), but milled for two different times (20 and 80 hours) and having particle size in micro[22] and nanometer domain, respectively. It was noticed that the heating has a distinct effect on the relative specific resistance of the two samples. Annealing at temperatures lower than about 500 K, results in a rapid decrease of the relative electrical resistivity for the 80 hours milled sample. This particular behaviour observed for nanometer sized sample at lower temperatures was also noted for other sub-microcrystalline metallic systems[48,52,53] and was explained by the relaxation of grain boundaries and by their transition from the stressed non-equilibrium state to equilibrium state. With a further increase in annealing temperature, relative electrical resistivity slowly decreases until 673 K and then, more rapidly until an almost constant value is reached, as a consequence of grain growth.

Fig. 7 Temperature dependence of the relative electrical resistivity of the Ag – 28 % Cu powders milled for two different times (20 hours and 80 hours)

Fig. 8 Relative electrical resistivity, Gibbs free energy function and crystallite size of the nanozised Ag – 28 % Cu powders as a function of temperature.

The variation of the relative electrical resistivity of the nanometer sized sample with the crystallite size and with the energy term is shown in Fig. 8. The slowly decreasing of the relative electrical resistivity around 500 K is correlated with the temperature dependence of both free energy and crystallite size (Fig. 4) which is non-monotonic and exhibits a minimum around this temperature. When the crystallite size is large, the free energy tends to the free energy of the coarsed-grained material and the resistivity decreases to a value which tends to remain constant.

The results presented here reveal the strong interplay of the energetic parameters with microstructure and properties in mechanically alloyed nanosized samples. The thermodynamic properties there are not only the driving force for grain growth process, but also may be used to explain the experimentally observed stability and the change of properties in a large domain of temperature.

Conclusions

In the present paper the thermodynamic properties, thermal expansion and electrical resistivity of the Ag – 28 % Cu nanopowders processed by mechanical alloying route have been investigated in the temperature range from ambient to 1048 K. The data were analyzed to make clear the parameters that favour stable nanostructured systems in mechanically alloyed samples with eutectic composition. For the first time, the relevant functions suitable for evaluation of the thermodynamic stability in particular temperature ranges associated with the grain growth process have been measured for the eutectic composition by drop calorimetry. It was shown that in mechanically alloyed nanosized sample, the thermodynamic properties there are not only the driving force for grain growth process, but also may be used to explain the experimentally observed stability and the change of properties in a large domain of temperature. The results obtained in the present study give for the first time evidence that, the concept of thermodynamic nanostructure stabilization is a real phenomenon for the mechanically alloyed Ag-Cu nanopowders with eutectic composition. Taking into account the importance of this concept in controlling grain size stability in nanocrystalline binary Ag-Cu systems, a comprehensive effort is needed to investigate the stability of the Ag-Cu nanoalloys with different Ag/Cu ratio. At this point further studies are in progress in our laboratory for a systematic investigation of the evolution of properties for different compositions in the Ag-Cu system processed by mechanically alloying route.

The thermodynamic properties together the thermal expansion results speak in the favour of the strong correlation between the thermal expansion and the energetic parameters controlling the growth process of nanometer-sized sample. The thermal expansion coefficient for the temperature range at which the free energy of the system reaches a local minimum with respect to the grain growth was 44×10^{-6} K^{-1}, which is about twice the value for bulk material.

Investigation of the electrical resistivity of the Ag - 28% Cu sample gives new arguments when speaking about the role of the energetic parameters in explaining the particular behaviour of Ag-Cu nanopowders with eutectic composition. The relative electrical resistivity was found to decrease with temperature, the general trend being strongly correlated with the evolution of the crystallite size and with non-monotonic variation of the energy term.

The comparison of the thermodynamic functions values obtained for the nanosized Ag – 28 % Cu sample with those of a microsized and bulk samples reveals the relationships between the energetic parameters and microstructure in mechanically alloyed samples. An increasing understanding of this correlation may allow exploring new possibilities for producing nanocrystalline materials by mechanical alloying process.

Notes and references

a *"Ilie Murgulescu" Institute of Physical Chemistry of the Romanian Academy, 202 Splaiul Independentei, 060021, Bucharest, Romania. Fax: + 40 21 3121147; Tel: + 40 21 3167912; E-mail: stanasescu2004@yahoo.com; stanasescu@icf.ro*
b *University of Craiova, Romania, 13 A.I. Cuza, 200585, Craiova, Romania. E-mail: oanagingu@yahoo.com*

References

1　H. H. Liebermann, *Rapidly solidified alloys: Processes, structures, properties, applications*, Marcel Dekker, New York, 1993.
2　C. Suryanarayana, *Non-equilibrium processing of materials*, Pergamon Press, Oxford, 1999.
3　B. Y. Tsaur, S. S. Lau and J. W. Mayer, *Appl. Phys. Lett.*, 1980, **36**, 823-826.
4　R. Enrique, F. Wu and P. Bellon, *Surf. Coat. Technol.*, 2002, **150**, 1-7.
5　H. W. Sheng, G. Wilde and E. Ma, *Acta Mater.*, 2002, **50**, 475-488.
6　H. Chen and J. M. Zuo, *Acta Mater.*, 2007, **55**, 1617-1628.
7　K. Upadhya, *Plasma synthesis and processing of materials*, The Minerals, Metals & Materials Society, Warrendale, 1993.
8　C. Suryanarayana, *Prog. Mater. Sci.*, 2011, **46**, 1-184.
9　L. Lu and M. O. Lai, *Mechanical alloying*, Kluwer Academic Publishers, Boston, 1998.
10　R. Ferrando, J. Jellinek and R. L. Johnston, *Chem. Rev.*, 2008, **108**, 845-910.
11　S. Chowdhury, V. R. Bhethanabotla and R. Sen, *Appl. Phys. Lett.*, 2009, **95**, 1311151-1311153.
12　S. J. Kim, E. A. Stach and C. A. Handwerker, *Appl. Phys. Lett.*, 2010, **96**, 1441011-1441013.
13　A. Ceylan, K. Jastrzembski and S. I. Shah, *Metall. Mater. Trans. A*, 2006, **37A**, 2033-2038.
14　T. Spassov, L. Lyubenova, Y. Liu, S. Bliznakov, M. Spassova and N. Dimitrov, *J. Alloys. Compd.*, 2009, **478**, 232-236.
15　M. Yang, C. Wu, C. Zhang and H. He, *Catal. Today*, 2004, **90**, 263-267.
16　E. Ma, *Prog. Mater. Sci.*, 2005, **50**, 413-509.
17　J. L. Murray, *Metall. Trans. A*, 1984, **15**, 261-268.
18　P. Duwez, R. H. Willens and W. Klement, *J. Appl. Phys.*, 1960, **31**, 1136-1137.
19　R. K. Linde, *J. Appl. Phys.*, 1966, **37**, 934.
20　K. Uenishi, K. F. Kobayashi, K. Y. Ishihara and P. H. Shingu, *Mater. Sci. Eng.*, 1991, **134**, 1342-1345.
21　J. H. He, H. W. Sheng and E. Ma, *Appl. Phys. Lett.*, 2001, **78**, 1343-1345.
22　A. Milea, O. Gingu, S. Preda, G. Sima, C. Nicolicescu and S. Tanasescu, *J. Alloy. Compd.*, 2015, **629**, 214-220.
23　T. Klassen, U. Herr and R. S. Averback, *Acta Mater.*, 1997, **45**, 2921-2930.
24　R. Najafabadi and D. J. Srolovitz, *J. Appl. Phys.*, 1993, **74**, 3144-3149.
25　E. Ma and M. Atzmon, *Mater. Chem. Phys.*, 1995, **39**, 249-267.
26　O. Gingu, C. Nicolicescu and G. Sima, *Solid State Phenom.*, 2012, **188**, 382-387.

27 H.P. Klug, L.E. Alexander, X-Ray Diffraction Procedure for Polycrystalline and Amorphous Materials, Wiley, New York, 1974

28 C. Y. Ho, M. W. Ackerman, K. Y. Wu, T. N. Havill, R. H. Bogaard, R. A. Matula, S. G. Oh and H. M. James, *J. Phys. Chem*, 1983, **12**, 183-322.

29 H. Gleiter, *Prog. Mater. Sci.*, 1989, **33**, 223-315.

30 A. Kelly and R. B. Nicholson, *Prog. Mater. Sci.*, 1963, **10**, 151-391.

31 M. Zhu, Z. F. Wu, M. Q. Zeng, L. Z. Ouyang and Y. Gao, *J. Mater. Sci.*, 2008, **43**, 3259-3266.

32 R. Najafabadi and D. J. Srolovitz, *J. Appl. Phys.*, 1993, **74**, 3144-3149.

33 H. A. Murdoch and C. A. Schun, *J. Mater. Res.*, 2013, **28**, 2154-2163.

34 T. Chookajorn, H. A. Murdoch and C. A. Schuh, *Science*, 2012, **337**, 951-954.

35 A. J. Detor and C. A. Schuh, *Acta Mater.*, 2007, **55**, 371-379.

36 M. Saber, C. C. Koch and R. O. Scattergood, *Mater. Res. Lett.*, 2014, 1-11

37 J. Weissmuller, P. Bunzel and G. Wilde, *Scripta Mater.*, 2004, **51**, 813-818.

38 C. C. Koch, R. O. Scattergood, M. Saber and H. Kotan, *J. Mater. Res.*, 2013, **28**, 1785-1791.

39 J. R. Trelewicz and C. A. Schuh, *Phys. Rev. B*, 2009, **79**, 0941121-09411213.

40 J. Weissmuller, *J. Mater. Res.*, 1994, **9**, 4-7.

41 J. Weissmuller, W. Krauss, T. Haubold, R. Birringer and H. Gleiter, *Nanostruct. Mater.*, 1992, **1**, 439-447.

42 C. E. Krill, H. Ehrhardt and R. Birringer, *Z. Metallkd*, 2005, **96**, 1134-1141.

43 B. S. Murty, M. K. Datta and S. K. Pabi, *Sadhana*, 2003, **28**, 23-45.

44 K. Lu, *Mater. Sci. Eng.*, 1996, **16**, 161-221.

45 H. Gleiter, *Acta Mater.,* 2000, **48**, 1-29.

46 M. K. Datta, *Synthesis and characterization of nanocristalline silicides by mechanical alloying in Fe-Ni-Si system*, PhD thesis, Indian Institute of Technology, Kharagpur, 2001.

47 C. Suryanarayana and C.C. Koch, *Hyperfine Interactions*, 2000, **130**, 5–44.

48 A. I. Gusev and A. A. Rempel, *Nanocrystalline materials*, Cambridge International Science Publishing, Cambridge, 2004.

49 M. Dubiel, S. Brunsch and L. Tröger, *J. Synchrotron Rad.*, 2001, **8**, 539-541

50 M. L. Sui, K. Lu, *Nanostruct. Mater.* 1995, **6**, 651-654

51 F. Cverna, ASM Ready Reference: Thermal properties of metals, ASM International, Materials Park, Ohio, USA, 2002

52 R. K. Islamgaliev, N. A. Akhmadeev, R. R. Mulyukov and R. Z. Valiev, *Phys. Stat. Sol. (a)*, 1990, **118**, K27-K29.

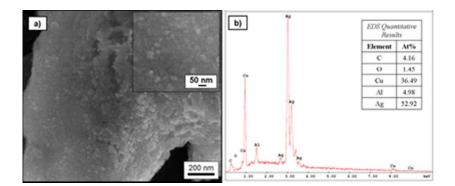53 K. Pekala and M. Pekala, *Nanostruct. Mater.*, 1995, **6**, 819-822.

Fig. 1 a) SEM micrograph and b) EDS analysis of the Ag-28% Cu alloy nanopowders ball milled for 80 hours
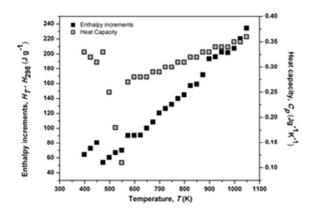34x14mm (300 x 300 DPI)

Fig. 2 Temperature dependence of the experimental enthalpy increments (HT-H298) and derived heat capacity (Cp) of the Ag – 28 % Cu nanopowders processed by mechanical alloying route
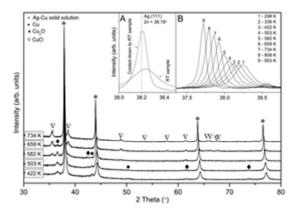24x19mm (300 x 300 DPI)

Fig. 3 In situ XRD of the Ag – 28 % Cu nanopowders during heating at successively increased temperature from RT to 973 K (Inset A: XRD patterns at room temperature before and after heating; Inset B: the evolution with temperature of the main diffraction line of the Ag-Cuss)
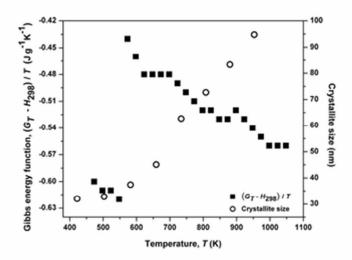24x16mm (300 x 300 DPI)

Fig. 4 Crystallite size (XRD measurements) and Gibbs energy function (drop calorimetry data) of the Ag - 28% Cu mechanical alloyed nanopowders as a function of temperature
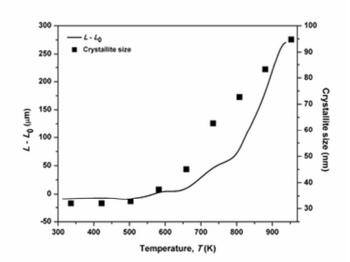
30x24mm (300 x 300 DPI)

Fig. 5 Temperature dependence of the thermal expansion and crystallite size of the Ag – 28 % Cu
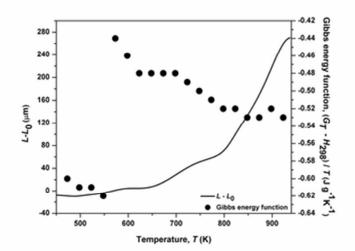nanopowders
29x23mm (300 x 300 DPI)

Fig. 6 Thermal expansion and Gibbs energy function of the Ag – 28 % Cu nanopowders as a function of temperature
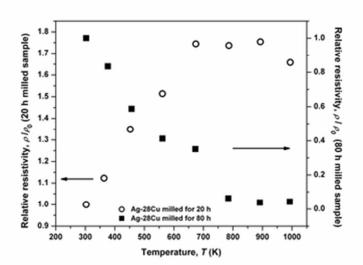29x23mm (300 x 300 DPI)

Fig. 7 Temperature dependence of the relative electrical resistivity of the Ag – 28 % Cu powders milled for
two different times (20 hours and 80 hours)
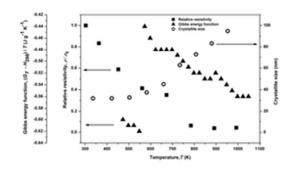30x24mm (300 x 300 DPI)

Fig. 8 Relative electrical resistivity, Gibbs free energy function and crystallite size of the nanozised Ag – 28 % Cu powders as a function of temperature.
24x15mm (300 x 300 DPI)

Table 1 Values of thermodynamic functions for Ag - 28% Cu mechanically alloyed nanopowders (80 hours milled) in comparison with the thermodynamic functions values for bulk and for a micrometer-sized mechanical alloyed sample (20 hours milled) with the same composition

T (K)	C_p (J g^{-1}K^{-1}) Sample milled for 80 hours	C_p (J g^{-1}K^{-1}) Sample milled for 20 hours*	C_p (J g^{-1}K^{-1}) Bulk	$S_T - S_{298}$ (J g^{-1} K^{-1}) Sample milled for 80 hours	$S_T - S_{298}$ (J g^{-1} K^{-1}) Sample milled for 20 hours*	$S_T - S_{298}$ (J g^{-1} K^{-1}) bulk	$-\dfrac{G_T - H_{298}}{T}$ (J g^{-1} K^{-1}) Sample milled for 80 hours	$-\dfrac{G_T - H_{298}}{T}$ (J g^{-1} K^{-1}) Sample milled for 20 hours*	$-\dfrac{G_T - H_{298}}{T}$ (J g^{-1} K^{-1}) Bulk
473	0.33	0.20	0.12	0.27	0.07	0.03	0.60	0.40	0.34
498	0.25	0.21	0.14	0.29	0.08	0.04	0.61	0.41	0.35
523	0.18	0.22	0.15	0.3	0.09	0.04	0.61	0.41	0.36
548	0.11	0.23	0.17	0.31	0.11	0.05	0.62	0.41	0.36
573	0.27	0.24	0.18	0.16	0.12	0.06	0.44	0.41	0.37
598	0.28	0.25	0.2	0.17	0.13	0.07	0.46	0.42	0.37
623	0.28	0.26	0.21	0.18	0.14	0.08	0.48	0.42	0.38
648	0.28	0.28	0.23	0.19	0.15	0.09	0.48	0.43	0.39
673	0.29	0.29	0.24	0.2	0.16	0.09	0.48	0.43	0.39
698	0.29	0.30	0.26	0.21	0.17	0.1	0.48	0.44	0.4
723	0.3	0.31	0.27	0.22	0.18	0.11	0.49	0.44	0.4
748	0.3	0.32	0.29	0.24	0.19	0.12	0.5	0.46	0.41
773	0.31	0.33	0.3	0.25	0.20	0.13	0.51	0.47	0.41
798	0.31	0.34	0.32	0.26	0.21	0.14	0.52	0.47	0.42
823	0.32	0.35	0.33	0.26	0.22	0.15	0.52	0.47	0.42
848	0.32	0.36	0.35	0.27	0.23	0.16	0.53	0.48	0.43
873	0.33	0.37	0.36	0.28	0.24	0.17	0.53	0.49	0.43
898	0.33	0.38	0.38	0.29	0.26	0.18	0.52	0.49	0.44
923	0.34	0.39	0.39	0.3	0.27	0.19	0.53	0.49	0.44
948	0.34	0.40	0.41	0.31	0.28	0.2	0.54	0.50	0.45
973	0.34	0.41	0.42	0.32	0.29	0.22	0.55	0.52	0.45
998	0.35	0.42	0.44	0.33	0.30	0.23	0.56	0.51	0.46
1023	0.35	0.43	0.45	0.34	0.31	0.24	0.56	0.52	0.46
1048	0.36	0.44	0.47	0.35	0.32	0.25	0.56	0.52	0.47

*Values calculated from the enthalpy data reported in ref.[22]